Am J Cancer Res 2023;13(11):5197-5217
www.ajcr.us /ISSN:2156-6976/ajcr0152200

Original Article

Protocadherin-1 serves as a prognostic biomarker and promotes pancreatic cancer progression by suppressing CD8$^+$ T cell infiltration through CCL5-CCR5 axis

Zhichen Jiang[1,2,3*], Shaobo Zhang[3*], Huiju Wang[1], Chunfang Hu[4], Li Li[1], Xiaohao Zheng[3], Yongrun Mu[3], Fangxia Wang[3], Yiping Mou[1], Mingyang Liu[3], Weiwei Jin[1]

[1]*Department of General Surgery, Devision of Gastroenterology and Pancreas, Zhejiang Provincial People's Hospital, Afliated People's Hospital, Hangzhou Medical College, Hangzhou 310014, Zhejiang, China;* [2]*The Second School of Clinical Medicine, Zhejiang Chinese Medical University, Hangzhou 310053, Zhejiang, China;* [3]*State Key Laboratory of Molecular Oncology, National Cancer Center/National Clinical Research Center for Cancer/Cancer Hospital, Chinese Academy of Medical Sciences and Peking Union Medical College, Beijing 100021, China;* [4]*Department of Pathology, National Cancer Center/National Clinical Research Center for Cancer/Cancer Hospital, Chinese Academy of Medical Sciences and Peking Union Medical College, Beijing 100021, China.* [*]*Equal contributors.*

Received July 13, 2023; Accepted October 4, 2023; Epub November 15, 2023; Published November 30, 2023

Abstract: Previous studies have shown that Protocadherins (PCDHs) enhance tumor proliferation, invasion, and metastasis; yet their role in pancreatic cancer (PC) progression and the tumor immune microenvironment remains unclear. This study aims to elucidate the role of PCDH1 in different cancer types, with a particular focus on its impact on immune suppression in PC. Utilizing data from TCGA, GTEx, and Gent2 databases, we assessed the expression of PCDH1 across various cancer types. The prognostic value of PCDH1 was demonstrated through Cox regression, Kaplan-Meier analysis, and ROC curve, while its relationship with gene mutations, tumor mutational burden (TMB), immune cell infiltration, and other clinical factors was investigated using Spearman correlation. Furthermore, the effect of PCDH1 on PC malignancy was experimentally validated by a series of in vitro and in vivo assays. Our results show a significant upregulation of PCDH1 in various tumor types, which is associated with poor prognosis, suggesting its potential application as an independent prognostic biomarker. Notably, in PC, PCDH1 exhibited significant associations with gene mutations, TMB, and immune cell infiltration. Clinical validations revealed a correlation between high PCDH1 expression and poor prognosis, coupled with a low level of CD8$^+$ T cell infiltration. Furthermore, both in vitro and in vivo experiments confirmed the role of PCDH1 in promoting PC cell proliferation and migration while inhibiting CD8$^+$ T cell recruitment through its modulation of CCL5-CCR5 axis. In conclusion, PCDH1 regulates the proliferation and migration of PC cells as well as CD8$^+$ T cell infiltration in PC. PCDH1 may serve as a prognostic biomarker in multiple tumor types.

Keywords: PCDH1, pancreatic cancer, CD8$^+$ T cell, CCL5, CCR5, immune

Introduction

Pancreatic cancer (PC) is a highly lethal digestive tract tumor with a 5-year survival rate of only 11%. According to the data from the American Cancer Society, PC is estimated to affect over 62,210 individuals, resulting in more than 49,830 deaths [1]. By 2040, PC is projected to surpass colorectal cancer as the second leading cause of cancer-related deaths in the United States [2]. The primary factors contributing to its poor prognosis are the lack of early symptoms, as well as its susceptibility to metastasis, recurrence, and treatment resistance [3-6].

Protocadherin 1 (PCDH1), a member of the δ1 subgroup (δ1-protocadherins) of the non-clustered PCDHs within the calmodulin family, has gained attention due to its involvement in various diseases. It possesses seven extracellular cadherin (EC) repeats, a transmembrane structural domain, and three evolutionarily conserved motifs in the intracellular tail [7, 8].

Recent studies have highlighted the crucial regulatory roles of PCDH1 in disease, including cancer. It regulates epithelial barrier function and activates TGF-β signaling through its interaction with SMAD3 [8-10]. Additionally, PCDH1 has been implicated in promoting PC progression by modulating NF-κB signaling [11].

Immunotherapy, which aims to activate the patient's immune system to eliminate tumor cells, has shown remarkable success in various cancers such as melanoma, lung cancer, and kidney cancer [12, 13]. However, its effectiveness is limited in certain cancers, including PC, due to an immunosuppressed TME, low tumor mutational burden (TMB), as well as impaired antigen processing and presentation [14-16]. TMB, defined as the number of somatic mutations per million base pairs of the genome, stands as a pivotal biomarker in tumors [17]. As a high TMB typically leads to the formation of more neoantigens, thereby activating antitumor immunity. This phenomenon is generally associated with better overall survival (OS) and more successful outcomes in immunotherapy [18, 19]. However, TMB level in PC is relatively low, registering at just 6.1 mut/Mb, which might constrain the effectiveness of immunotherapies [17]. Additionally, the unique characteristics of TME in PC, where tumor cells comprise only 20% of the overall tumor environment, while the dense extracellular matrix forms a physical barrier, contribute to the redistribution of immune cells and intricate crosstalk among TME cells [20, 21]. These factors collectively limit the efficacy of immunotherapy in PC.

Despite the investigation of PCDH1 in certain benign and malignant diseases, there is a lack of comprehensive studies encompassing the entire spectrum of cancer. Moreover, studies on the interaction between PCDH1 and TME are limited. In this study, we conducted differential expression analysis of PCDH1 across multiple cancer types and performed prognostic analysis using publicly available databases. We further focused investigating on the role of PCDH1 in regulating PC cell phenotype and as a potential prognostic biomarker. We also explored the relationship of PCDH1 expression levels with gene mutations, TMB, and neoantigen signatures as well as alterations in the methylation status of PCDH1 in PC. More importantly, we experimentally validated our findings obtained from bioinformatics analyses. Our data highlight the significance of PCDH1 as a prognostic marker in various cancers, including PC.

Materials and methods

Source of data

RNA sequencing data, clinicopathology data, and mutation data for PAAD were obtained from the TCGA database. Additionally, we utilized several other databases for our analyses, including the Gene Expression Database for Normal and Tumor Tissues2 (Gent2) database (http://gent2.appex.kr/gent2/), the Tumor Immune Estimation Resource (TIMER) database, The University of Alabama at Birmingham Cancer data analysis Portal (UALCAN database), the Gene Expression Profiling Interactive Analysis (GEPIA) database (http://gepia.cancer-pku.cn/), the Comprehensive Analysis on Multi-Omics of Immunotherapy in Pan-cancer (CAMOIP) database [22], the UALCAN database for DNA methylation changes in the PCDH1 promoter, and the STRING database (https://string-db.org/cgi/input?sessionId=bL2ZI4D08-8fF) for simulating protein-protein interaction (PPI) networks. The TISIDB database was used to predict the relationship of PCDH1 with chemokines, immune subtypes, and neoantigens [23]. The abbreviations and full names of the cancer types are provided in **Table 1**.

Differential expression analysis

The Gent2 database is a publicly accessible platform that compiles the gene expression profiles of normal and tumor tissues in various gene expression datasets [24]. In this study, we initially examined the expression of PCDH1 in GPL570 dataset across multiple cancer types. Subsequently, we utilized the TIMER database to analyze the differential expression of PCDH1 in the TCGA dataset [25, 26]. Due to the limited availability of certain tumor-normal paired samples in the TCGA dataset, we employed the GEPIA database to analyze the differential expression of PCDH1 by combining data from TCGA and GTEx database [27] (Table S1). To assess the differential protein levels of PCDH1 between PC and normal samples, we utilized the UALCAN database containing Clinical Proteomics Tumor Analysis Consortium (CPTAC) data for this analysis.

Table 1. Abbreviations and full name

Abbreviation	Full title
ACC	Adrenocortical carcinoma
BLCA	Bladder Urothelial Carcinoma
BRCA	Breast invasive carcinoma
CESC	Cervical squamous cell carcinoma and endocervical adenocarcinoma
CHOL	Cholangiocarcinoma
COAD	Colon adenocarcinoma
DLBC	Lymphoid Neoplasm Diffuse Large B-cell Lymphoma
ESCA	Esophageal carcinoma
GBM	Glioblastoma multiforme
HNSC	Head and Neck squamous cell carcinoma
KICH	Kidney Chromophobe
KIRC	Kidney renal clear cell carcinoma
KIRP	Kidney renal papillary cell carcinoma
LAML	Acute Myeloid Leukemia
LGG	Brain Lower Grade Glioma
LIHC	Liver hepatocellular carcinoma
LUAD	Lung adenocarcinoma
LUSC	Lung squamous cell carcinoma
MESO	Mesothelioma
OV	Ovarian serous cystadenocarcinoma
PAAD	Pancreatic adenocarcinoma
PCPG	Pheochromocytoma and Paraganglioma
PRAD	Prostate adenocarcinoma
READ	Rectum adenocarcinoma
SARC	Sarcoma
SKCM	Skin Cutaneous Melanoma
STAD	Stomach adenocarcinoma
TGCT	Testicular Germ Cell Tumors
THCA	Thyroid carcinoma
THYM	Thymoma
UCEC	Uterine Corpus Endometrial Carcinoma
UCS	Uterine Carcinosarcoma
UVM	Uveal Melanoma
NSCLC	Non Small Cell Lung Cancer
TCGA	The Cancer Genome Atlas
GTEx	Genotype-Tissue Expression
PC	Pancreatic cancer
TMB	Tumor mutation burden
IHC	Immunohistochemistry
CCL5	C-C motif chemokine ligand 5
CCR5	C-C motif chemokine receptor 5
EC	Extracellular calmodulin
TGF-β	Transforming growth factor-β
SMAD3	SMAD family member 3
NF-κB	Nuclear factor kappa-B
TME	Tumor microenvironment
DFS	Disease-free survival

PFS	Progression-free survival
AUC	Area under the curve
GO	Gene Ontology
KEGG	Kyoto Encyclopedia of Genes and Genomes
PPI	Protein-protein interaction
ssGSEA	Single-sample gene set enrichment analysis
ATCC	The American Type Culture Collection
PCR	Polymerase Chain Reaction
shRNA	Short hairpin RNA
qRT-PCR	Quantitative real-time PCR
WB	Western blotting
OS	Overall survival
DEGs	Differentially expressed genes
CCL2	C-C motif chemokine ligand 2
CM	Conditioned medium
IDO2	Indoleamine 2,3-dioxygenase 2
GM-CSF	Granulocyte-macrophage colony-stimulating factor
MHC-I	Major histocompatibility complex class I
APCs	Antigen-presenting cells
CXCL9	C-X-C motif chemokine ligand 9
CXCL10	C-X-C motif chemokine ligand 10
CXCL11	C-X-C motif chemokine ligand 11
CXCL13	C-X-C motif chemokine ligand 13
CX3CL1	CX3C-chemokine ligand 1
CAFs	Cancer-associated fibroblasts
ECM	Extracellular matrix
HIF2	Hypoxia-inducible factors-2

Prognostic analysis

We utilized the GEPIA database to assess the relationship between PCDH1 expression and prognosis across various cancer types, including overall survival (OS) and recurrence-free survival (RFS). Multifactorial and univariate COX regression analyses were conducted to determine the independent prognostic value of PCDH1. Additionally, we evaluated the prognostic value of PCDH1 for PC using progression-free survival (PFS) and AUC. To perform relevant prognostic analyses, we employed the "survival", "survminer", and "timeROC" packages.

Functional enrichment analysis and PPI networks

We divided patients into PCDH1 high and low expression groups based on the median value of PCDH1 expression. Differentially expressed genes (DEGs) were identified using the "limma" package with criteria of $|\log2FC| \geq 1$ and FDR < 0.01. Enrichment analysis of these DEGs was conducted using the "clusterProfiler" package for GO and KEGG. PPI analysis of the DEGs was performed using the STRING database. The top 10 core genes were identified using the CytoHubba plug-in in Cytoscape software.

Relationship between PCDH1 expression and immune cell infiltration

To assess the degree of immune cell infiltration in each patient within TCGA-PAAD, we employed the "CIBERSORT" algorithm. The correlation between PCDH1 expression and the level of immune cell infiltration was determined using the "ggplot2" and "ggpubr" packages. Additionally, ssGSEA was performed using the "limma", "GSVA", and "GSEABase" packages to analyze changes in immune pathways in the PCDH1 high and low expression groups [28]. The TISIDB database was utilized to predict the relationship of PCDH1 with chemokines and immune subtypes. The CAMOIP database was employed to analyze the relationship between PCDH1 and neoantigens.

Relationship of PCDH1 with TMB and DNA methylation

Somatic mutation data were obtained from the TCGA database and analyzed using the "maftools" R package. TMB was calculated for each patient, and patients were separated into high and low TMB groups using the median TMB value. Kaplan-Meier (K-M) survival analysis was performed by integrating TMB with PCDH1 expression levels. The UALCAN database was used to analyze the variation in PCDH1 promoter methylation in PC.

Cell culture, plasmids, and lentiviral infection

Human pancreatic ductal adenocarcinoma (PDAC) cell lines (AsPC-1, MiaPaCa-2, BxPC-3, SW1990, and PANC-1) and 293T cell line were obtained from ATCC. $CD8^+$ T cells were kindly provided by Dr. Chenze Zhang (the Institute of Laboratory Animal Sciences, Chinese Academy of Medical Sciences). All cell lines were STR-identified and confirmed to be free of mycoplasma as determined by the MycoBlue Mycoplasma Detector (Vazyme). The cells were cultured as described previously [29-31].

PCR amplification was performed to obtain the full-length cDNA of PCDH1, and the resulting product was cloned into the pCMV-MCS-3Flag vector (Obio technology). The shRNA of PCDH1 was cloned into the pSLenti-U6-shRNA-CMV-EGFP-F2A-Puro-WPRE vector (Obio technology). Lentivirus was produced in 293T cells using a second-generation packaging system consisting of psPAX2 (Addgene) and pMD2.G (Addgene). Transfection was carried out using Lipofectamine™ 3000 (Thermo Fisher Scientific). The shRNA sequences can be found in Table S2. Virus-containing medium was collected 48 hours after transfection, filtered through a 0.45 μm pore size Millex® PVDF syringe filter (Merck), and was used to infect PC cells in the presence of 8 mg/mL polybrene (Sigma-Aldrich) for 48 hours. The infected cells were further selected by 2 mg/mL puromycin (Sangon Biotech) or 400 mg/mL G418 (MCE) for seven days to establish stable cell lines.

Tissue microarray and immunohistochemistry (IHC) staining

Tissue microarray slides were constructed using tumor tissues obtained from 86 PC patients who underwent surgery at the Zhejiang Provincial People's Hospital between January 1, 2016, and January 1, 2022. The study was conducted in accordance with the principles stated in the Declaration of Helsinki and approved by the Ethics Committee of Zhejiang Provincial People's Hospital (approval number: QT2022268). Before surgery, all patients provided written informed consent and received no specific treatment.

IHC of the slides was performed using PCDH1 antibody (SANTA CRUZ BIOTECHNOLOGY; working dilution 1:4000) and CD8 antibody (Proteintech; working dilution 1:1500). Two experienced pathologists independently scored the staining results.

RNA isolation and qRT-PCR

Total RNA was extracted using the PureLinkTM RNA Mini Kit (Thermo Fisher Scientific), and cDNA was synthesized using the HiScript® III RT SuperMix for qPCR (+gDNA wiper) (Vazyme). SYBR™ Green (Thermo Fisher Scientific) was used for qRT-PCR analysis. Changes in mRNA levels were analyzed using the $2^{-\Delta\Delta CT}$ method with GAPDH as the internal reference. Table S2 provides the primer sequences used in this study.

CCK-8 assay, colony formation assay, and wound healing assay

For CCK-8 Assay, PC cells were seeded in a 96-well plate (3000 cells/well) with 100 μl of complete medium. At 0, 24, 48, 72, and 96 hours of culture, 10 μl of the reagent from CCK-8 Cell Counting Kit (Vazyme) was added to each well and incubated for 1 hour at 37°C, protected from light. The absorbance was measured at 450 nm using a Thermo Scientific Multiskan FC plate reader (Thermo Fisher Scientific).

For colony formation assay, PC cells were seeded at a density of 500 cells per well in six-well plates with 2 ml of complete medium. The medium was changed every 3 days, and after 2 weeks of culture, the cells were fixed with 4% formaldehyde (methanol-free, Biosharp) for 30 minutes and stained with 1% crystal violet ammonium oxalate solution (Solarbio) for 30 minutes.

For wound healing assay, PC cells were seeded in a six-well plate and allowed to grow to 100% confluence. Scratches were made using a 200 μl pipette tip, and the culture medium was changed to 1% FBS-containing medium. Photographs were taken at 0 and 24 hours using a 40× magnification, and the healing area was calculated using image analysis software.

Mouse xenograft tumor model

Six-week-old male BALB/c nude mice were obtained from Charles River Laboratory and randomly divided into experimental groups. PC cells (5 * 10^6 cells/100 ul) stably expressing plasmids for PCDH1 knockdown, PCDH1 overexpression, or control vector were subcutaneously injected into the dorsal side of the mice. Tumor growth was monitored every 4 days for 27 days. Tumor volume was calculated using the formula: 0.5 * length * $width^2$. At the end of the study, the tumors were surgically removed and weighed. Two individuals (operator and recorder) performed the procedures as a group, with the operator unaware of the group assignment.

Western blot (WB) analysis

Standard WB protocol was used as reported previously [30]. The total cell extracts were prepared, and WB was performed using indicated antibodies. The following antibodies were used: Beta Actin (Abcam; working dilution: 1:1000) and PCDH1 (SANTA CRUZ BIOTECHNOLOGY; working dilution: 1:400).

CD8+ T cell recruitment assay

After PC cells reached 80-90% confluence, the culture medium was replaced with fresh medium, and cells were cultured for 48 hours before the medium was collected as conditioned medium (CM), which was then filtered using a 0.45 μm pore size Millex® PVDF syringe filter (Merck) and added to the lower chamber of a Transwell system (Corning). CD8+ T cells (3 * 10^5/200 μl) were added to the upper chamber and incubated at 37°C in 5% CO_2 for 48 hours. The cells migrated to the lower side of the chamber were then fixed in 4% formaldehyde (methanol-free, Biosharp) for 30 minutes and stained with 1% crystal violet ammonium oxalate solution (Solarbio) for another 30 minutes.

The single-cell data analysis

The single-cell data used in this study were obtained from the datasets by Peng et al. [32], and we focused on treatment-naïve PDAC patients. To preprocess the single-cell data, we employed Seurat (v4.2.0) to filter, downscale, cluster, and annotate the data, following the methodology described in the original article [32]. Specifically, we stratify the CD8+ subpopulation within the T cell population based on CD8 expression greater than 0 and then analyzed the correlation between the overall expression of PCDH1 and the proportion of CD8+ T cells in the ductal epithelial cells of PC.

Statistical analysis

Statistical analysis was conducted using GraphPad Prism V.8 for Windows (GraphPad Software), R (V.4.2.3) and SPSS 22.0. The data were presented as mean ± SD. Independent Student's t-test or one-way ANOVA was employed to analyze the data. Correlation analysis was performed using Spearman correlate analysis. Statistical significance was defined as *P*-values < 0.05, and all tests were two-sided.

Result

Examination of PCDH1 expression across various cancer types

We first analyzed PCDH1 mRNA expression level in human tumor and matched normal samples using the HG-U133 microarray (GPL570 platform) obtained from the Gent2 database (**Figure 1A**). PCDH1 expression was found to be upregulated in various cancer types, such as PC, ovarian cancer, thyroid cancer, bladder cancer, adrenal carcinoma, and bone cancer, compared to normal samples. However, the downregulated PCDH1 expression was observed in other cancer types such as brain cancer, colon cancer, head and neck cancer, kidney cancer, liver cancer, lung cancer, skin cancer, pharynx cancer, vulva cancer, tongue cancer, and endometrial cancer. Subsequently, we employed the TIMER2.0 database to validate the differential expression of PCDH1 between tumor and normal samples. As depicted in **Figure 1B**, PCDH1 exhibited differential expression in various cancer types. Specifically, it was upregulated in BLCA, BRCA, CHOL, KICH, LIHC, PAAD, PCPG, PRAD, STAD, and THCA, whereas it was downregulated in

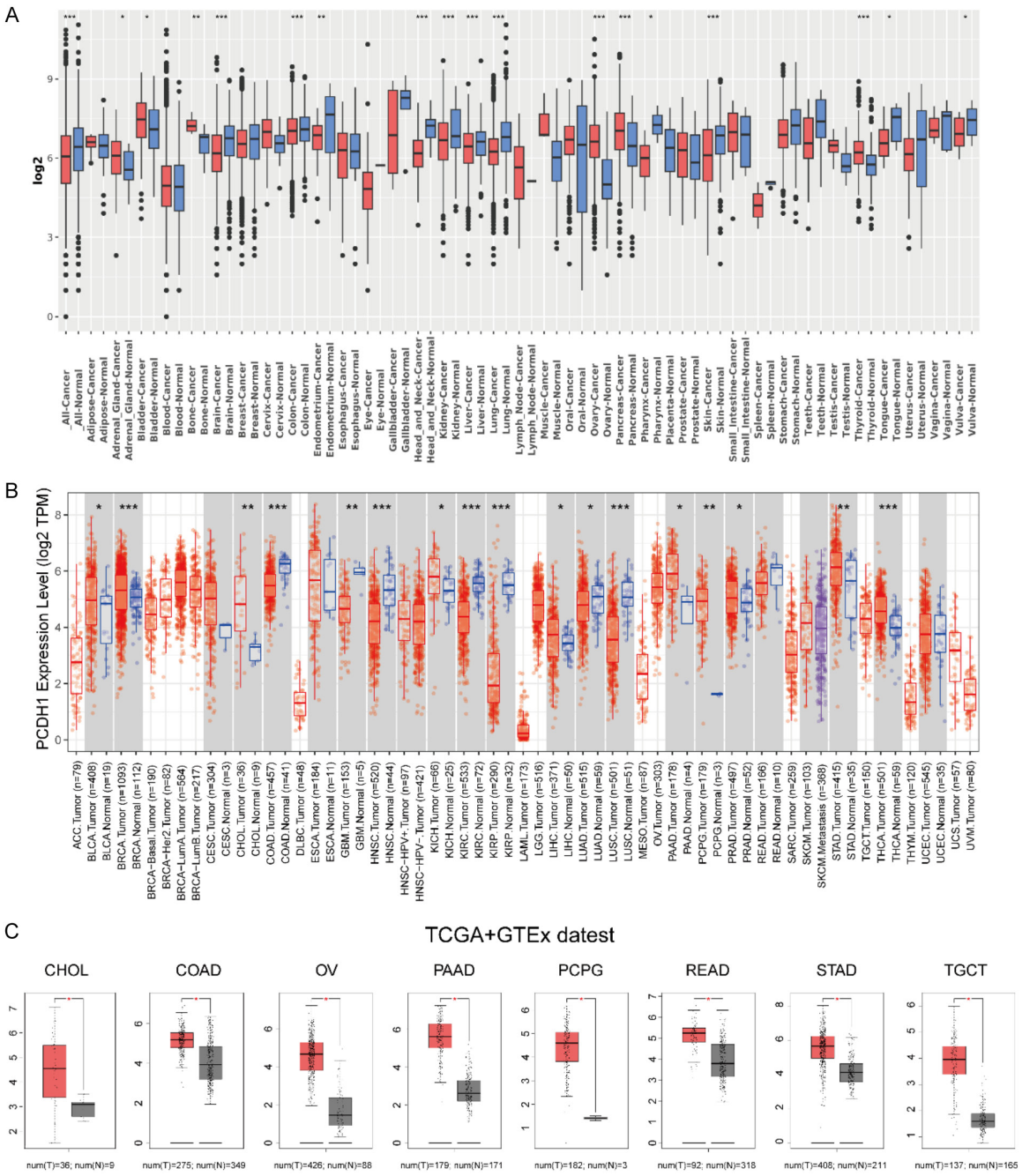

Figure 1. PCDH1 expression across various cancer types. A: PCDH1 expression between tumor tissues and normal tissue from Gent2 database across various cancer types. B: PCDH1 expression between tumor tissues and normal tissue from TCGA database across various cancer types. C: PCDH1 expression between tumor tissues and normal tissue from TCGA and GTEx database across various cancer types (*: $P < 0.05$; **: $P < 0.01$; ***: $P < 0.001$). Abbreviations. TCGA: The Cancer Genome Atlas; GTEx: Genotype-Tissue Expression.

COAD, GBM, HNSC, KIRC, KIRP, LUAD, and LUSC. Lastly, due to the limited availability of normal samples in TCGA datasets, we supplemented the study with normal tissue expression data obtained from the GTEx dataset, which served as a control group. Subsequently, we retrieved the mRNA expression profile of PCDH1 in human tumors using the GEPIA website. Our analysis revealed that PCDH1 was upregulated in CHOL, COAD, OV, PAAD, PCPG, READ, STAD, and TGCT when compared to normal samples (**Figure 1C**), while it was downregulated in HNSC, KIRP, LAML, LUSC, and SKCM (Figure S1A).

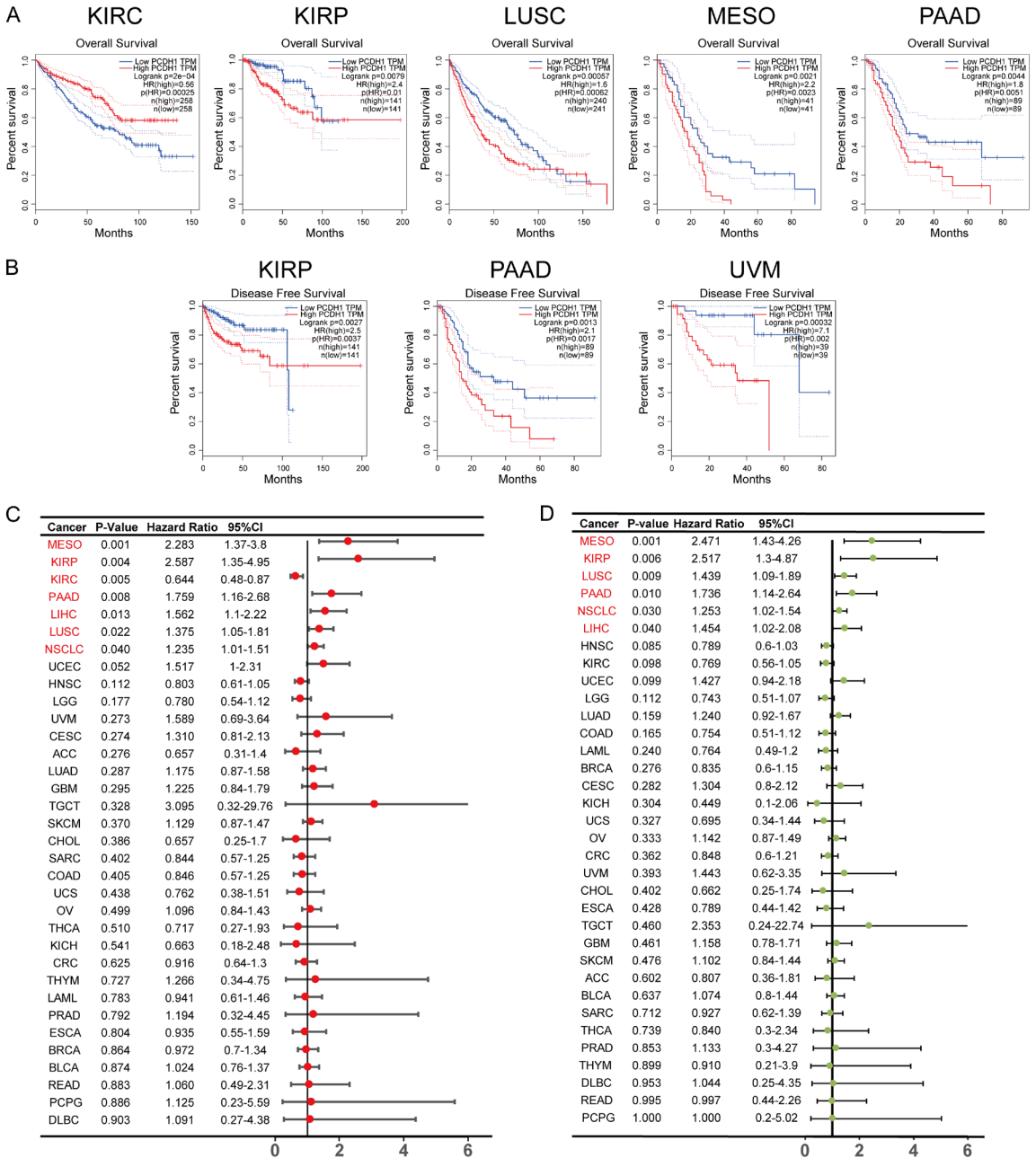

Figure 2. Survival analysis of PCDH1 across various cancer types. A: Kaplan-Meier curves showing OS across various cancer types. Only significant results were shown. B: Kaplan-Meier curves showing DFS across various cancer types. Only significant results were shown. C: Forest map shows the univariate cox regression results of PCDH1 for OS in TCGA. The red cancer is the significant result. D: Forest map shows the univariate cox regression results of PCDH1 for OS in TCGA. The red cancer is the significant result. Abbreviations. OS: Overall survival; DFS: Disease-free survival; TCGA: The Cancer Genome Atlas.

Survival analysis of PCDH1 across various cancer types

We next employed K-M curves to examine the association of PCDH1 expression with OS and RFS across various cancer types (**Figure 2A**, **2B**). Among these cancer types, we observed a negative correlation between PCDH1 expression and OS in KIRC, KIRP, LUSC, MESO, and PAAD. Furthermore, KM survival analysis revealed a significant correlation between high PCDH1 expression levels and reduced RFS in KIRP, PAAD, and UVM. Additionally, we utilized univariate and multivariate COX regression

models to assess the potential of PCDH1 as an independent prognostic marker across various cancer types (**Figure 2C**, **2D**). In the univariate COX regression model, the high expression of PCDH1 was associated with a poor prognosis of MESO, KIRP, KIRC, PAAD, LIHC, LUSC, and NSCLC, which was supported by multivariate Cox regression model, suggesting the prognosis-predictive value of PCDH1 for these cancer types.

Differential expression and prognostic analysis of PCDH1 in PC

Since the above analyses demonstrated the different expression pattern of PCDH1 among different cancer types, we focused our study on the function of PCDH1 in PC. We first confirmed a substantial upregulation of PCDH1 protein in PC compared to matched normal samples (**Figure 3A**). Additionally, we examined the difference in disease free survival (DFS) between the high and low PCDH1 expression groups and observed a correlation between high PCDH1 expression and poor DFS (**Figure 3B**). Furthermore, the ROC curves demonstrated that PCDH1 exhibited AUC greater than 0.6 in predicting the 1-, 3-, and 5-year OS in PAAD patients (**Figure 3C**). Taken together, we found that PCDH1 was significantly overexpressed in PC and was associated with an unfavorable prognosis. Moreover, we conducted microarray IHC to validate the effect of PCDH1 expression on prognosis. As shown in **Table 2**, although the baseline characteristics were similar between the high- and low-PCDH1 expression groups, the survival analysis demonstrated a significantly decreased OS in patients with high PCDH1 expression (**Figure 3D**). A representative image of high and low PCDH1 expression was shown in **Figure 3E** and **3F**, respectively.

Functional enrichment analysis

To explore the biological functions of PCDH1, we carried out functional enrichment analysis. First, GO/KEGG analysis on the DEGs between the high and low PCDH1 expression groups revealed that the genes upregulated in the PCDH1 high expression group were primarily enriched in pathways associated with transmembrane transport and ligand regulation (**Figure 4A-C**), suggesting that PCDH1 may play a regulatory role in cell-cell communication and substance transport processes. Next, PPI analysis on these DEGs identified MUC1, ITGB4, SNAP25, PPL, ERBB2, MUC16, EVPL, GRIA2, ITGA6, and MET as the top ten core genes (**Figures 4D** and S1B).

Relationship of PCDH1 expression with gene mutation, TMB, and DNA methylation

We further conducted a comprehensive analysis of gene mutations in the high and low PCDH1 expression groups in the TCGA-PAAD dataset and found a higher probability of gene mutations in the high PCDH1 expression group than in the low expression group (92.4% vs 71.08%) (**Figure 5A**, **5B**). Specifically, the four most mutated genes were KRAS (80% vs 43%), TP53 (68% vs 45%), SMAD4 (23% vs 20%), and CDKN2A (27% vs 10%). Moreover, we explored the relationship between PCDH1 expression and TMB and observed higher TMB levels in the high PCDH1 expression group (**Figure 5C**), indicating a positive correlation between them (R=0.37, *P*=2.3E-06) (**Figure 5D**). To evaluate the impact of TMB combined with PCDH1 expression on patient outcomes, we plotted a K-M curve using OS as the endpoint and found that the high TMB and high PCDH1 expression combination group had the worst OS (**Figure 5E**). We also investigated the DNA methylation levels of PCDH1 in PC and adjacent normal tissues and observed a significantly higher PCDH1 promoter methylation in PC (**Figure 5F**).

PCDH1 promotes the progression of PC cells in vitro and in vivo

To validate the findings from our bioinformatics analyses, we conducted a series of biological experiments to determine the function of PCDH1 in PC progression. First, we assessed the mRNA levels of PCDH1 in five PC cell lines, Aspc-1, BXPC-3, MiaPaCa-2, SW1990, and PANC-1, and found a highest PCDH1 level in SW1990 while a lowest level in PANC-1, which was consistent with the protein expression levels as determined by WB (**Figure 6A**). Subsequently, we successfully generated SW1990 stable cell lines with PCDH1 knockdown (SW1990-SH1, SW1990-SH2, and SW1990-SH3) as well as PANC-1 stable cell line with PCDH1 overexpression (PANC1-ORF). The efficiency of knockdown and overexpression was further determined at the mRNA and protein levels (**Figure 6B**). Next, we used PCDH1

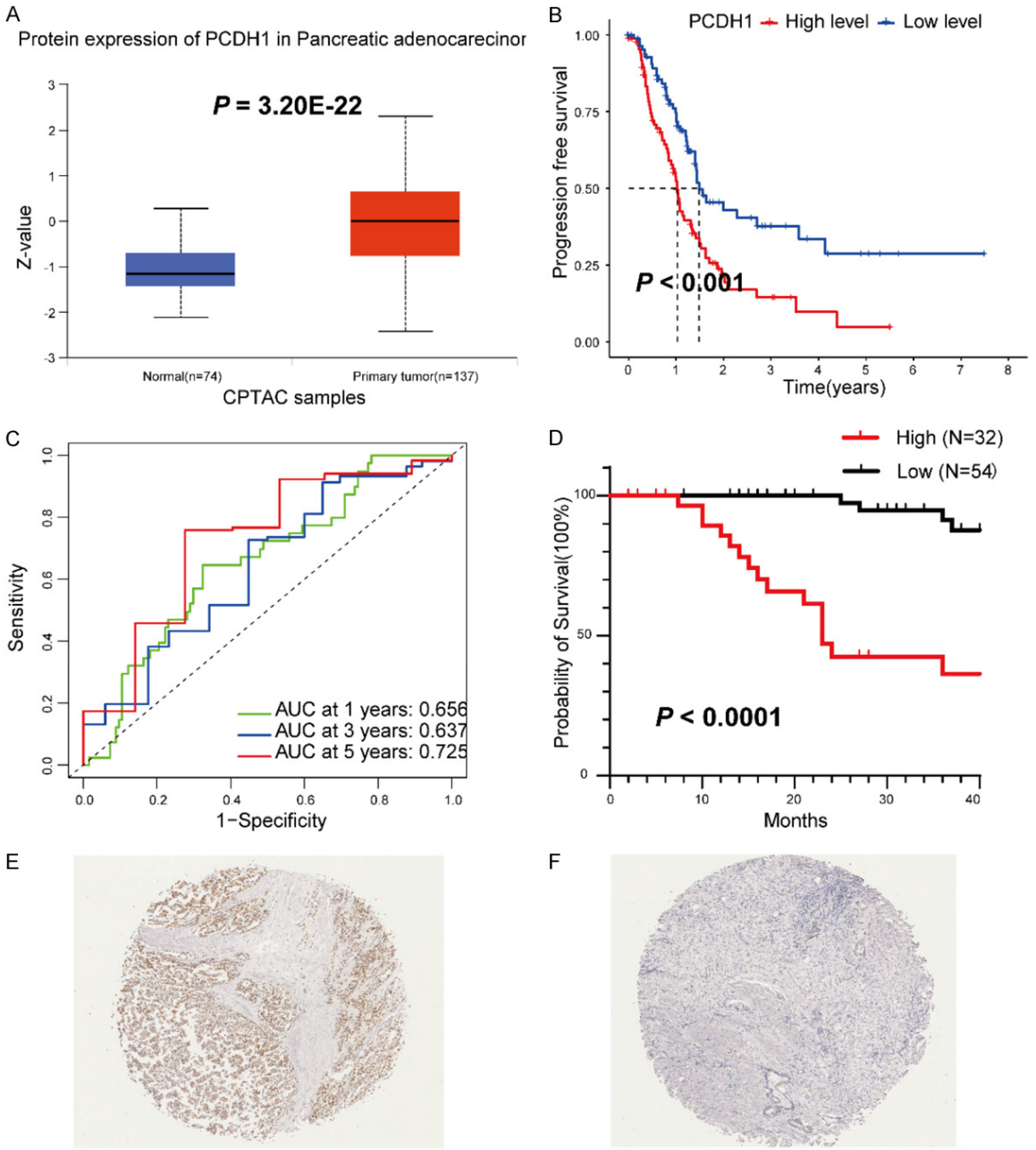

Figure 3. Differential expression and prognostic analysis of PCDH1 in PC. A: The PCDH1 protein level in PAAD was examined using the CPTAC dataset. B: Kaplan-Meier curves showing DFS in PAAD. C: The ROC of PCDH1 predict 1, 3, and 5-year survival in PAAD patients. D: Kaplan-Meier curves showing OS in PC. E: Representative IHC staining for high PCDH1 expression. F: Representative IHC staining for low PCDH1 expression. Abbreviations. PAAD: Pancreatic adenocarcinoma; DFS: Disease-free survival; OS: Overall survival; IHC: Immunohistochemistry; PC: Pancreatic cancer; CPTAC: Clinical Proteomics Tumor Analysis Consortium.

knockdown strains (SW1990-SH1, SW1990-SH2) and PCDH1 overexpression strains (PANC1-ORF) to evaluate the impact of altered PCDH1 expression on PC cell phenotype. CCK-8 assays demonstrated that the downregulated PCDH1 expression significantly inhibited SW1990 cell growth, while the enhanced expression of PCDH1 promoted the proliferation of PANC-1 cells (**Figure 6C**). Colony formation assays further supported this conclusion (**Figure 6D**). Moreover, wound healing assay demonstrated that PCDH1 overexpression sig-

Table 2. Clinicopathological features and correlation with PCDH1 expression

		PCDH1		Total (%)	*P* value
		Low, no. cases (%)	High, no. cases (%)		
Age (years)	≥ 65	31 (57.4)	17 (53.1)	48 (55.8)	0.699
	< 65	23 (42.6)	15 (46.9)	38 (44.2)	
Sex	Male	32 (59.3)	17 (53.1)	49 (57)	0.579
	Female	22 (40.7)	15 (46.9)	37 (43)	
T classification	I	2 (3.7)	2 (6.3)	4 (4.7)	0.221
	II	43 (79.6)	20 (62.5)	63 (73.3)	
	III	9 (16.7)	10 (31.3)	19 (22.1)	
Lymphatic metastasis	Yes	21 (38.9)	14 (43.8)	35 (40.7)	0.657
	No	33 (61.1)	18 (56.3)	51 (59.3)	
Hypertension	Yes	21 (38.9)	12 (17.5)	33 (38.4)	0.898
	No	33 (61.1)	20 (62.5)	53 (61.6)	
Diabetes	Yes	9 (16.7)	8 (25)	17 (19.8)	0.348
	No	45 (83.3)	24 (75)	69 (80.2)	
Location	Head	31 (57.4)	18 (56.3)	49 (57)	0.917
	Body and tail	23 (42.6)	14 (43.8)	37 (43)	
BMI	< 18.5	7 (13)	9 (28.1)	16 (18.6)	0.179
	18.5-24	29 (53.7)	16 (50)	45 (52.3)	
	≥ 24	18 (33.3)	7 (21.0)	25 (29.1)	

BMI: Body Mass Index.

nificantly enhanced while knockdown significantly impaired the migration ability of PANC-1 and SW1990 cells, respectively (**Figure 6E**, **6F**).

To further investigate the physiological function of PCDH1 in PC in vivo, we used xenograft tumor model in nude mice. Stable SW1990 cells with PCDH1 knockdown (SW1990-SH1) and stable PANC-1 cell with PCDH1 overexpression (PANC1-ORF) as well as their respective controls were subcutaneously injected into the flank of mice, and the tumor growth was monitored every 4 days for 27 days. The data showed that the tumor weight and volume were significantly smaller in the PCDH1 knockdown group compared to the control group (**Figure 6G-I**), whereas the overexpression of PCDH1 resulted in a larger tumor in weight and volume (**Figure 6J-L**), indicating the growth-promoting role of PCDH1 in PC.

Effect of PCDH1 on immune surveillance

To further understand the function of PCDH1 in tumor progression, we conducted a comprehensive analysis of the immunological profile associated with PCDH1. Utilizing the CIBERSORT algorithm, we identified a negative correlation between PCDH1 expression and $CD8^+$ T cells (R=-0.32, *P*=0.006) (**Figure 7A**), suggesting that patients with high PCDH1 expression might have a poor prognosis due to a reduced infiltration of $CD8^+$ T cells. We further investigated their relationship at both the single cell as well as tissue levels and observed a negative correlation between PCDH1 expression in ductal epithelial cells and the proportion of $CD8^+$ T cells (**Figure 7B**). This finding was subsequently validated at the tissue level, where PCDH1 expression exhibited a negative correlation with CD8 expression (**Figure 7C**). Furthermore, $CD8^+$ T cell recruitment assays confirmed the inhibitory effect of PCDH1 on $CD8^+$ T cell recruitment (**Figure 7D**, **7E**).

Chemokines play a pivotal role in regulating immune cell infiltration, and our analysis revealed a negative correlation between PCDH1 expression and CCL2 and CCL5 levels in PC cells (**Figures 7F**, S2A, S2B), suggesting that CCL2 and CCL5 might mediate the effect of PCDH1 on $CD8^+$ T cell infiltration. Further experimental validation showed that the downregulation of PCDH1 expression resulted in a significant elevation of CCL5 expression (**Figure 7G**). Subsequently, we examined the expres-

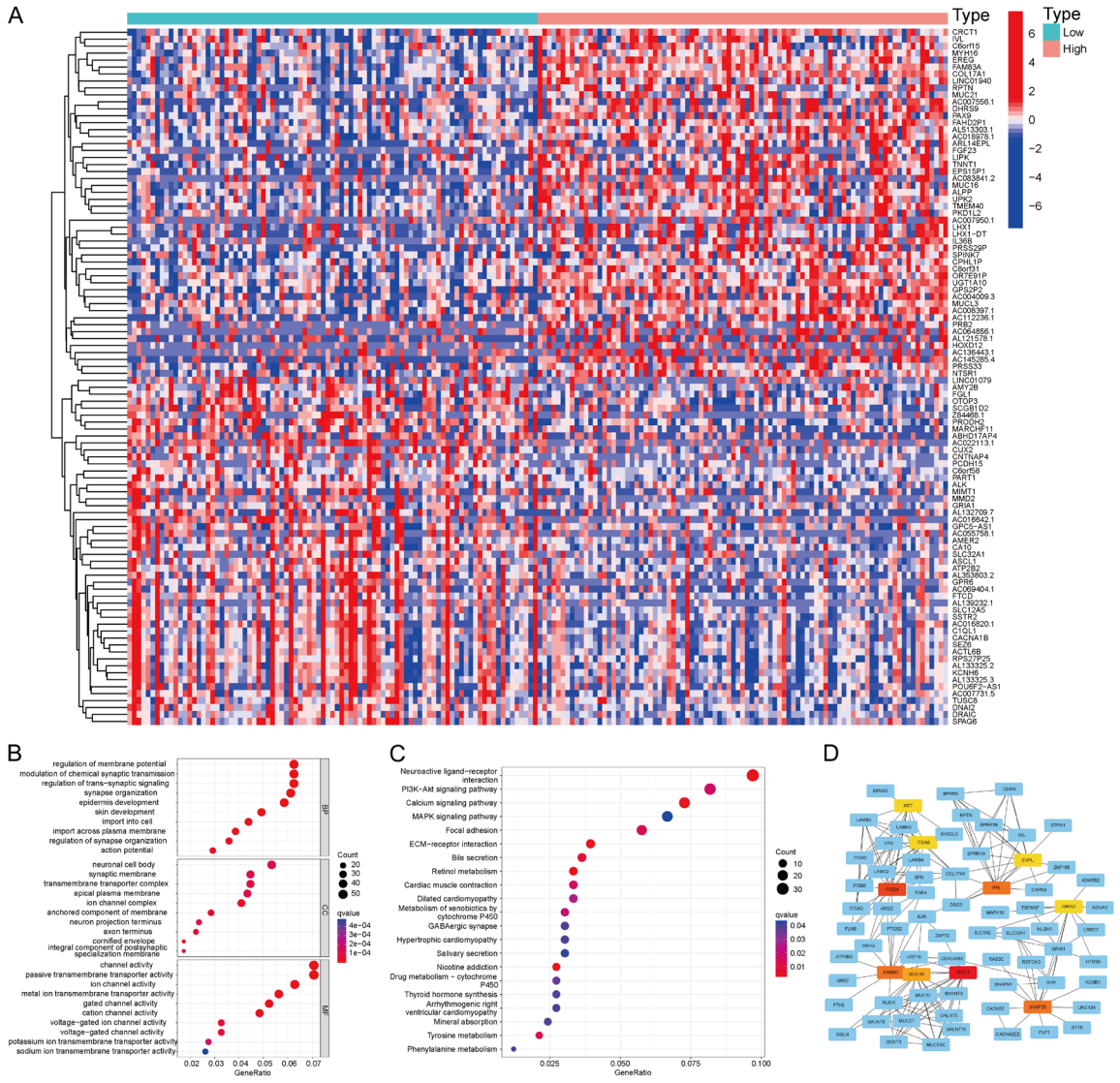

Figure 4. Functional enrichment analysis of PCDH1. A: Heat map of differentially expressed genes in high-low expression group of PCDH1. B: GO enrichment analysis of differentially expressed genes in high and low PCDH1 groups. C: KEGG enrichment analysis of differentially expressed genes in high and low PCDH1 groups. D: PPI analysis of differentially expressed genes in high and low expression group of PCDH1. Abbreviations. GO: Gene Ontology; KEGG: Kyoto Encyclopedia of Genes and Genomes; PPI: Protein-protein interaction.

sion of CCR5 in CD8⁺ T cells that were treated with CM from PCDH1 knockdown SW1990-SH cells and, intriguingly, observed a substantial upregulation of CCR5 expression (**Figure 7H**). Collectively, these data suggest that PCDH1 may impede CD8⁺ T cell infiltration through modulating the CCL5-CCR5 axis.

We further conducted immune function analysis and found that the PCDH1 high expression group displayed higher scores in MHC_class_I and Type_I_IFN_Response but lower scores in Type_II_IFN_Response, Cytoolytic_activity, and T_cell_co-stimulation (**Figure 8A**). Importantly, we investigated the correlation between PCDH1 and neoantigens as well as genes associated with immunotherapy. The PCDH1 high expression group displayed a higher proportion of neoantigens (**Figure 8B**), and PCDH1 expression was positively correlated with most genes associated with immune checkpoint inhibitor therapy (except IDO2) (**Figure 8C**), although TIDE scoring system showed no significant difference in predicting

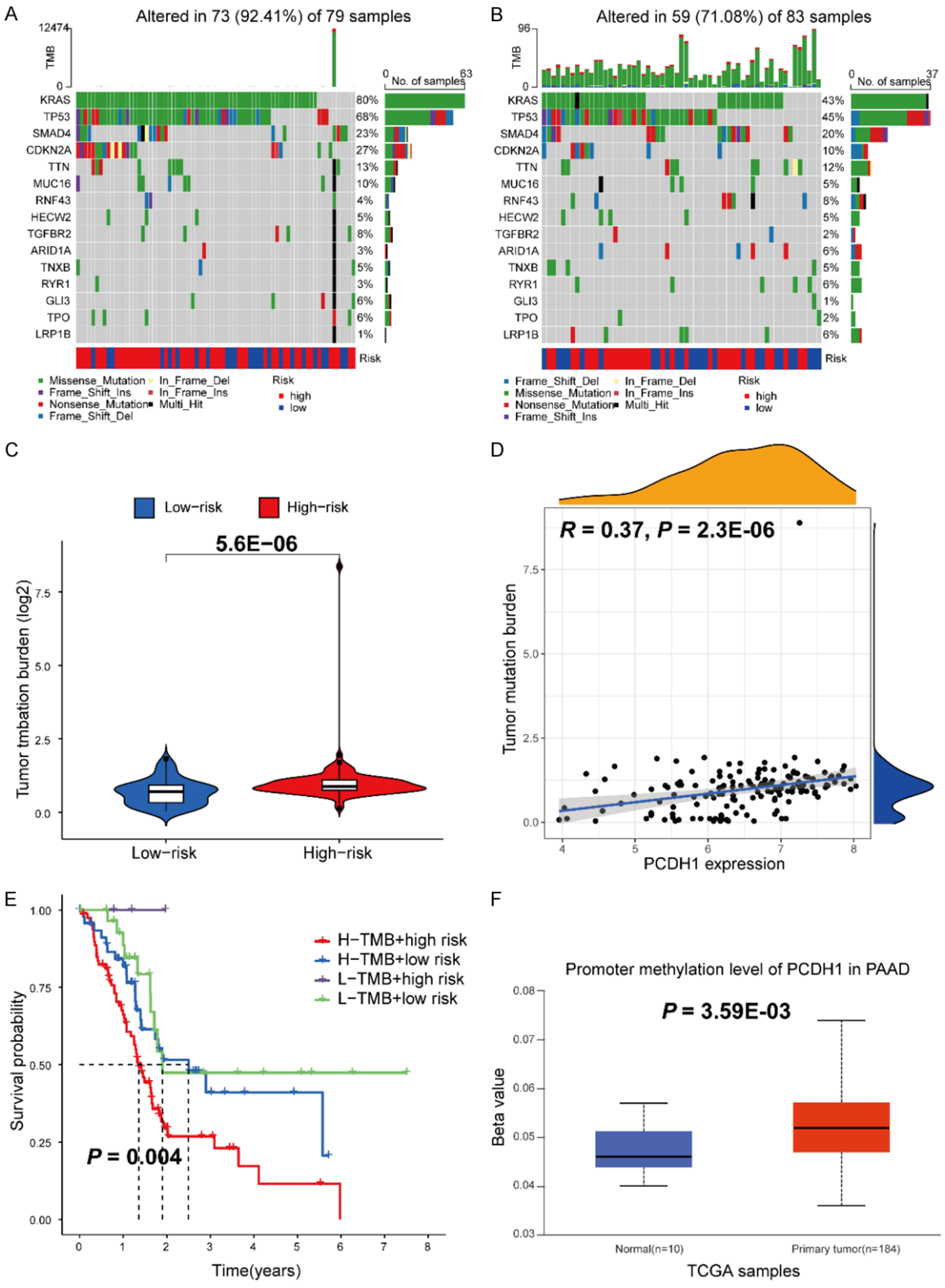

Figure 5. Relationship between PCDH1 expression and gene mutation, TMB, and DNA methylation. A: Gene mutation in high PCDH1 expression group. B: Gene mutation in low PCDH1 expression group. C: TMB was higher in the group with high PCDH1 expression in PAAD. D: Correlations between PCDH1 expression and TMB in PAAD. E: Kaplan-Meier curves showing OS in PC. F: DNA methylation analysis of PCDH1 in PAAD. Abbreviations. TMB: Tumor mutation burden; OS: Overall survival; PAAD: Pancreatic adenocarcinoma.

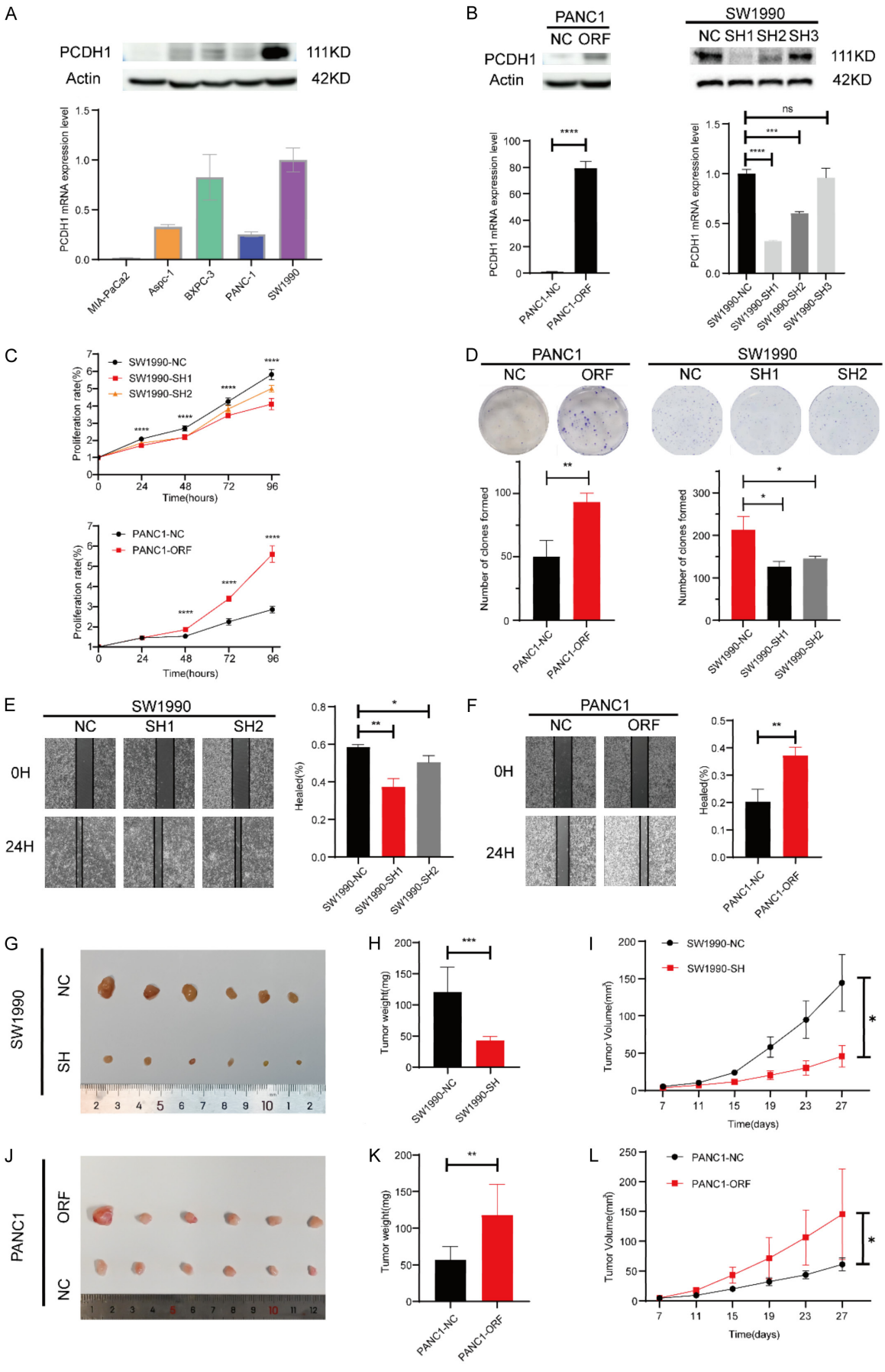
A
PCDH1
Actin
111KD
42KD
PCDH1 mRNA expression level
MIA-PaCa2
Aspc-1
BXPC-3
PANC-1
SW1990
B
PANC1
NC ORF
SW1990
NC SH1 SH2 SH3
PCDH1
Actin
111KD
42KD
PCDH1 mRNA expression level
PANC1-NC
PANC1-ORF
SW1990-NC
SW1990-SH1
SW1990-SH2
SW1990-SH3
ns
C
SW1990-NC
SW1990-SH1
SW1990-SH2
Proliferation rate(%)
Time(hours)
PANC1-NC
PANC1-ORF
D
PANC1
NC ORF
SW1990
NC SH1 SH2
Number of clones formed
E
SW1990
NC SH1 SH2
0H
24H
Healed(%)
F
PANC1
NC ORF
0H
24H
Healed(%)
G
SW1990
NC
SH
H
Tumor weight(mg)
SW1990-NC
SW1990-SH
I
SW1990-NC
SW1990-SH
Tumor Volume(mm³)
Time(days)
J
PANC1
ORF
NC
K
Tumor weight(mg)
PANC1-NC
PANC1-ORF
L
PANC1-NC
PANC1-ORF
Tumor Volume(mm³)
Time(days)

Figure 6. PCDH1 promotes the progression of PC cells in vivo and in vitro. A: WB, and qRT-PCR used to reflect PCDH1 expression in different PC cell lines. B: WB, and qRT-PCR used to reflect changes in PCDH1 expression levels after following lentiviral transfection. C: CCK8 assay responding to SW1990, PANC1 proliferation. D: Colony formation assays response to SW1990, PANC1 proliferation. E, F: Wound-healing assay response to SW1990, PANC1 migration ability. G: Representative images depicting the tumors formed in the SW1990-NC/SW1990-SH groups. H: Following 27 consecutive days of tumor volume measurement, mice in the SW1990-NC/SW1990-SH groups were euthanized, and their body weight was recorded. I: Tumor proliferation curves were plotted based on measurements taken over the course of 27 consecutive days in the SW1990-NC/SW1990-SH groups. J: Representative images depicting the tumors formed in the PANC1-NC/PANC1-ORF groups. K: Following 27 consecutive days of tumor volume measurement, mice in the PANC1-NC/PANC1-ORF groups were euthanized, and their body weight was recorded. L: Tumor proliferation curves were plotted based on measurements taken over the course of 27 consecutive days in the PANC1-NC/PANC1-ORF groups. Abbreviations. WB: Western blotting; qRT-PCR: Quantitative real-time PCR.

the effectiveness of immunotherapy (**Figure 8D**).

Finally, we classified the immune subtypes of PAAD into C1 (wound healing), C2 (IFN-gamma-dominant), C3 (inflammatory), C4 (lymphocyte-depleted), C5 (immune-quiet), and C6 (TGF-b-dominant). Interestingly, the PCDH1 high-expression group was predominantly associated with the C1 subtype (**Figure 8E**).

Discussion

In this study, we conducted a comprehensive analysis of PCDH1 from differential expression analysis across various cancer types to its prognosis predicting value and identified PCDH1 as a potential independent prognostic marker in several tumors. We further focused our study on elucidating the impact of PCDH1 in PC progression. To validate PCDH1 as a prognostic marker for PC, we performed clinical validation and demonstrated its association with patient outcomes. Additionally, we conducted functional enrichment analysis of DEGs in the high and low PCDH1 expression groups to elucidate the underlying molecular mechanisms. Furthermore, we explored the relationship of PCDH1 expression with gene mutations, TMB, and neoantigen signature in the PCDH1 high and low expression groups. We also investigated changes in PCDH1 methylation levels. These analyses provided valuable information on the genetic and epigenetic alterations associated with PCDH1 in PC. Based on these, we performed in vitro and in vivo experiments to validate the role of PCDH1 in promoting the progression of PC cells. Finally, we analyzed in detail the regulation of PCDH1 on the immune feature of PC and performed some experimental validation.

PCDH1 has been implicated as a potential asthma susceptibility gene in previous studies. It is believed to influence the function of the epithelial barrier by affecting intercellular tight junctions and adhesion junctions, suggesting a role in intercellular signaling and substance exchange. Our functional enrichment analysis of differentially expressed genes in PCDH1 high and low expression groups supports the regulatory role of PCDH1 in ion channel activity and other processes. These findings suggest that PCDH1 may impact the crosstalk between PC cells and TME cells.

PC is considered as a “cold tumor” with limited immune cell infiltration, particularly potent immune cells. Effective immune cells, such as $CD8^+$ T cells and NK cells, play a crucial role in anti-tumor responses [33, 34]. Infiltration of $CD8^+$ T cells has been associated with better prognosis in PC patients [35]. PC cells exert significant control over the infiltration and function of immune cells by secreting various substances [15]. For instance, PC cells can produce indoleamine 2,3-dioxygenase to degrade tryptophan, leading to T cell apoptosis and loss of function [36]. They can also secrete GM-CSF to promote the recruitment of immunosuppressive bone marrow cells [37]. Additionally, PC cells can upregulate PD-L1 expression by increasing the stability of PD-L1 mRNA through activating the RAS pathway [38]. Furthermore, PC cells possess the ability to impact antigen presentation. For example, they can induce autophagy and downregulate the surface levels of MHC-I in tumor cells, thereby inhibiting antigen presentation [39]. Moreover, PC cells exhibit a high expression of CD47, which acts as an inhibitory signal for APCs and further hinders antigen presentation [40]. These influences of PC cells on immune cells highlight their pivotal role in modulating immune responses. In our study, we observed a correlation between high PCDH1 expression and $CD8^+$ T cell infiltration suppression. Chemokines are a class of

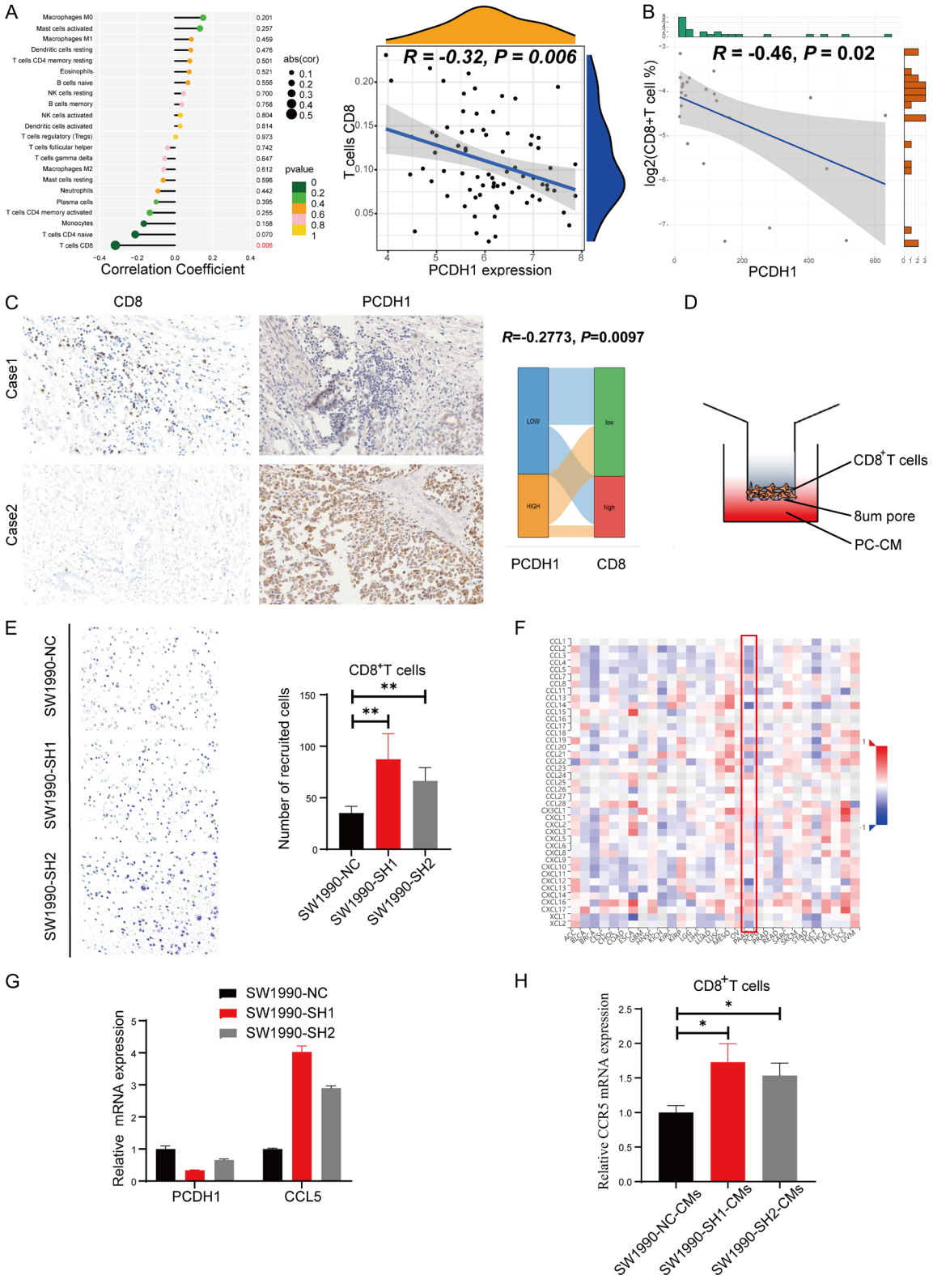

Figure 7. PCDH1 regulates CD8⁺ T cell infiltration via the CCL5-CCR5 axis. A: Analysis of the TCGA database revealed a negative correlation between PCDH1 expression and CD8⁺ T cell infiltration. B: At the single-cell level, PCDH1 expression in ductal epithelial cells exhibited a negative correlation with the proportion of CD8⁺ T cells. C: At the tissue level, PCDH1 expression is negatively correlated with CD8 expression. Case 1 represents a patient exhibiting high

CD8 expression and low PCDH1 expression, while Case 2 corresponds to a patient with low CD8 expression and high PCDH1 expression. D: Schematic representation of the CD8+ T cell recruitment assay. E: CM from SW1990-SH1 and SW1990-SH2 cells recruited significantly more CD8+ T cells compared to SW1990-NC cells. F: Analysis of chemokines associated with PCDH1 expression across various cancer types (PAAD results highlighted in red box). G: The downregulation of PCDH1 expression led to a significant increase in CCL5 expression in PC cells. H: Treatment of CD8+ T cells with CM from SW1990-SH1 and SW1990-SH2 cells resulted in higher CCR5 expression levels compared to SW1990-NC cells. Abbreviations. CM: Conditioned medium; CCL5: C-C motif chemokine ligand 5; CCR5: C-C motif chemokine receptor 5; TCGA: The Cancer Genome Atlas; IHC: immunohistochemistry.

relatively small proteins with molecular weights ranging from 8 to 14 kDa [41]. Extensive research has identified their involvement in diverse biological processes such as angiogenesis, wound healing, inflammatory diseases, and cancer progression. Among all known chemokines, CXCL9, CXCL10, CXCL11, CXCL13, CX3CL1, CCL2, and CCL5 exhibit a specific affinity for T-cell infiltration [42-44]; hence, we focused on these chemokines, particularly on the correlation of PCDH1 expression with CCL2 and CCL5 levels ($R < -0.3$). To validate this association, we conducted qRT-PCR analysis and observed that the suppressed PCDH1 expression led to an increased CCL5 expression. Consistently, CD8+ T cells that were treated with CM from PCDH1-depleted PC cells exhibited an elevated CCR5 expression. These findings suggest that PCDH1 may affect CD8+ T cell infiltration through regulating CCL5 expression.

Our study also revealed significantly higher TMB and neoantigen levels in the PCDH1 high expression group compared to the PCDH1 low expression group, suggesting that patients with high PCDH1 expression may benefit from immunotherapy. The correlation between PCDH1 and immune checkpoint-related genes further supports this notion. However, our predicted immunotherapeutic effect did not show a significant difference between the PCDH1 high and low expression groups, which might be due to the unique TME of PC, characterized by the low infiltration of immune effector cells and the abundance of other cell types. For instance, cancer-associated fibroblasts (CAFs) in the extracellular matrix secrete CDH11, leading to an increased stromal activation, collagen, and fibronectin expression, as well as the inhibition of T and B cell infiltration [45]. Additionally, HIF2 in CAFs enhances the recruitment of immunosuppressive macrophages, further suppressing the response to immune checkpoint blockade [46].

While this study has shed light on the function of PCDH1 in PC progression, it has some limitations. First, some of the findings were derived from bioinformatics analysis using public databases, which requires further validation using external samples or experimentally. Second, although this study identified an oncogenic effect of PCDH1 on PC and revealed the relationship between PCDH1 and CD8+ T cell infiltration, further studies are needed to elucidate the underlying mechanisms by which PCDH1 regulates PC progression. Third, since the regulatory mechanism of PCDH1 expression on CD8+ T cells in PC was primarily explored through bioinformatics analysis and in vitro experiments, additional studies are required to further understand the regulatory role of PCDH1 on CD8+ T cells in PC.

Conclusion

Our study provides compelling evidence suggesting that PCDH1 may predict the prognosis of patients with various tumor types, including PC. Notably, we observed elevated levels of PCDH1 methylation in PC. Additionally, the PCDH1 high expression group exhibited significantly higher rates of gene mutations, TMB, and neoantigen presentation compared to the low expression group. hrough a series of in vivo and in vitro experiments, we successfully confirmed the tumor-promoting role of PCDH1 in PC. Importantly, our findings also indicate that PCDH1 may impact the prognosis of PC patients by modulating the expression of the chemokine CCL5, which could potentially influence the infiltration of CD8+ T cells.

Acknowledgements

We are grateful to Dr. Chenze Zhang (the Institute of Laboratory Animal Sciences, Chinese Academy of Medical Sciences, China) for the CD8+ T cells lines. We are grateful for the staff and administrators of the public database utilized in this study. This study was supported

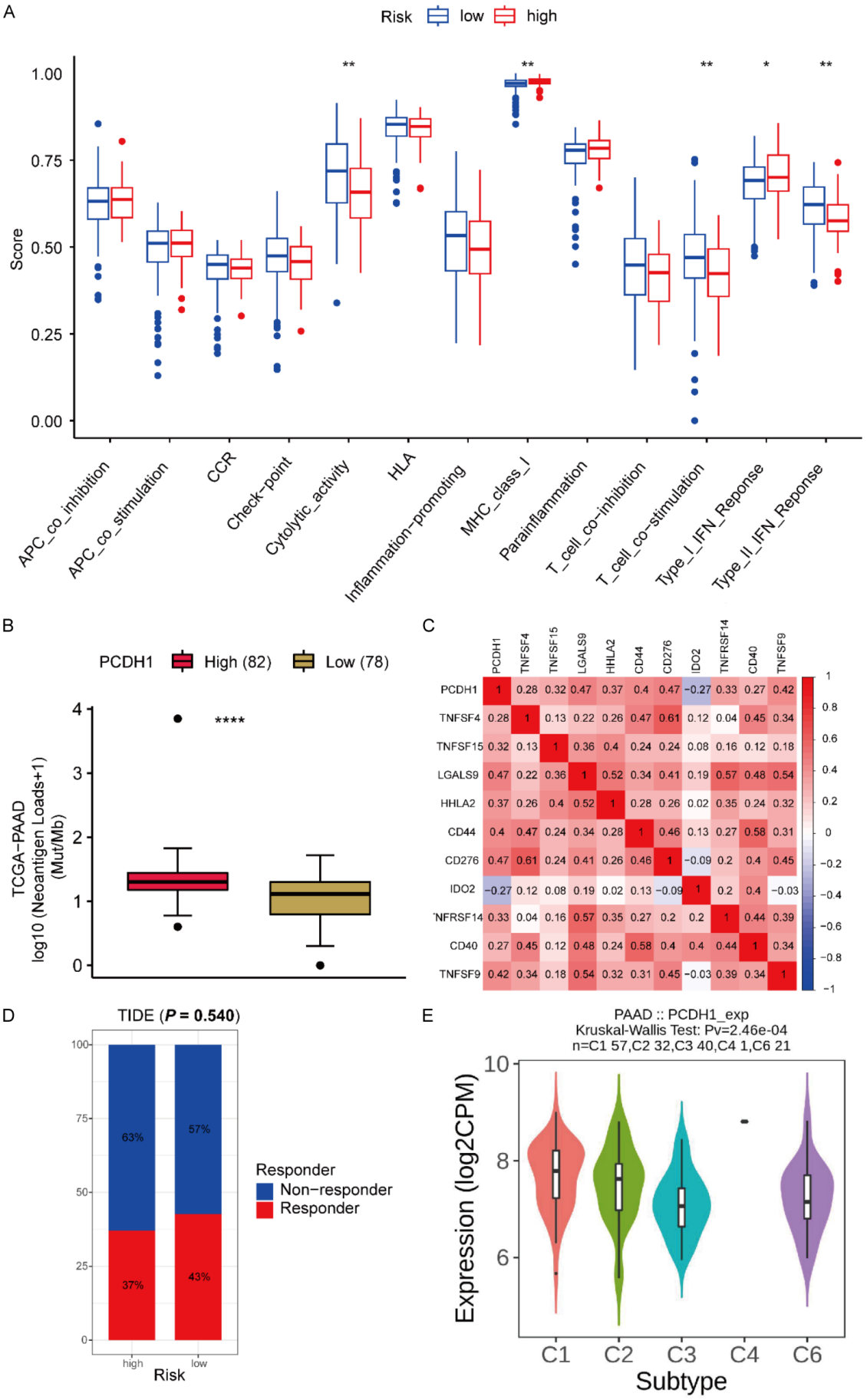
A
Risk low high
Score
1.00
0.75
0.50
0.25
0.00
**
**
**
*
**
APC_co_inhibition
APC_co_stimulation
CCR
Check-point
Cytolytic_activity
HLA
Inflammation-promoting
MHC_class_I
Parainflammation
T_cell_co-inhibition
T_cell_co-stimulation
Type_I_IFN_Reponse
Type_II_IFN_Reponse
B
PCDH1 High (82) Low (78)
****
TCGA-PAAD
log10 (Neoantigen Loads+1)
(Mut/Mb)
C
PCDH1 TNFSF4 TNFSF15 LGALS9 HHLA2 CD44 CD276 IDO2 TNFRSF14 CD40 TNFSF9
D
TIDE (P = 0.540)
63%
57%
37%
43%
high
low
Risk
Responder
Non−responder
Responder
E
PAAD :: PCDH1_exp
Kruskal-Wallis Test: Pv=2.46e-04
n=C1 57,C2 32,C3 40,C4 1,C6 21
Expression (log2CPM)
C1
C2
C3
C4
C6
Subtype

Figure 8. Immunological characterization of PCDH1. A: Comparative analysis of immune function between the high and low PCDH1 expression groups. B: Higher neoantigen ratio observed in the PCDH1 high expression group compared to the PCDH1 low expression group. C: Heat map illustrating the correlation between PCDH1 expression and immune checkpoint-related genes. D: Prediction of immunotherapy efficacy in the PCDH1 high and low expression groups. E: Relationship between PCDH1 expression and immune subtypes.

by the Scientific Research Fund of the National Health Commission of China, the Key Health Science and Technology Program of Zhejiang Province (WKJ-ZJ-2201), the Key Project of Social Welfare Program of Zhejiang Science and Technology Department, 'Lingyan' Program (2022C03099), and the Zhejiang Provincial Basic Technology Foundation of China (Grant No. LGC20H160003).

Disclosure of conflict of interest

None.

Address correspondence to: Drs. Yiping Mou and Weiwei Jin, Department of General Surgery, Devision of Gastroenterology and Pancreas, Zhejiang Provincial People's Hospital, Afliated People's Hospital, Hangzhou Medical College, Hangzhou 310014, Zhejiang, China. Tel: +86-13605818289; E-mail: yipingmou@126.com (YPM); Tel: +86-13738054378; E-mail: jinww@zju.edu.cn (WWJ); Mingyang Liu, State Key Laboratory of Molecular Oncology, National Cancer Center/National Clinical Research Center for Cancer/Cancer Hospital, Chinese Academy of Medical Sciences and Peking Union Medical College, Beijing 100021, China. Tel: +86-17681924541; E-mail: liumy@cicams.ac.cn

References

[1] Siegel RL, Miller KD, Fuchs HE and Jemal A. Cancer statistics, 2022. CA Cancer J Clin 2022; 72: 7-33.

[2] Rahib L, Wehner MR, Matrisian LM and Nead KT. Estimated projection of US cancer incidence and death to 2040. JAMA Netw Open 2021; 4: e214708.

[3] Halbrook CJ, Lyssiotis CA, Pasca di Magliano M and Maitra A. Pancreatic cancer: advances and challenges. Cell 2023; 186: 1729-1754.

[4] Jiang Z, Wang H, Mou Y, Li L and Jin W. Functions and clinical applications of exosomes in pancreatic cancer. Mol Biol Rep 2022; 49: 11037-11048.

[5] Wood LD, Canto MI, Jaffee EM and Simeone DM. Pancreatic cancer: pathogenesis, screening, diagnosis, and treatment. Gastroenterology 2022; 163: 386-402, e381.

[6] William C, Wangmo C and Ranjan A. Unravelling the application of machine learning in cancer biomarker discovery. Cancer Insight 2023; 2: 1-8.

[7] Kim SY, Yasuda S, Tanaka H, Yamagata K and Kim H. Non-clustered protocadherin. Cell Adh Migr 2011; 5: 97-105.

[8] Jangra RK, Herbert AS, Li R, Jae LT, Kleinfelter LM, Slough MM, Barker SL, Guardado-Calvo P, Román-Sosa G, Dieterle ME, Kuehne AI, Muena NA, Wirchnianski AS, Nyakatura EK, Fels JM, Ng M, Mittler E, Pan J, Bharrhan S, Wec AZ, Lai JR, Sidhu SS, Tischler ND, Rey FA, Moffat J, Brummelkamp TR, Wang Z, Dye JM and Chandran K. Protocadherin-1 is essential for cell entry by new world hantaviruses. Nature 2018; 563: 559-563.

[9] Vishnubalaji R and Alajez NM. Epigenetic regulation of triple negative breast cancer (TNBC) by TGF-β signaling. Sci Rep 2021; 11: 15410.

[10] Faura Tellez G, Vandepoele K, Brouwer U, Koning H, Elderman RM, Hackett TL, Willemse BW, Holloway J, Van Roy F, Koppelman GH and Nawijn MC. Protocadherin-1 binds to SMAD3 and suppresses TGF-beta1-induced gene transcription. Am J Physiol Lung Cell Mol Physiol 2015; 309: L725-L735.

[11] Ye Z, Yang Y, Wei Y, Li L, Wang X and Zhang J. PCDH1 promotes progression of pancreatic ductal adenocarcinoma via activation of NF-kappaB signalling by interacting with KPNB1. Cell Death Dis 2022; 13: 633.

[12] Zhu H, Li T, Du Y and Li M. Pancreatic cancer: challenges and opportunities. BMC Med 2018; 16: 214.

[13] Balachandran VP, Beatty GL and Dougan SK. Broadening the impact of immunotherapy to pancreatic cancer: challenges and opportunities. Gastroenterology 2019; 156: 2056-2072.

[14] Li X, Gulati M, Larson AC, Solheim JC, Jain M, Kumar S and Batra SK. Immune checkpoint blockade in pancreatic cancer: trudging through the immune desert. Semin Cancer Biol 2022; 86: 14-27.

[15] Ullman NA, Burchard PR, Dunne RF and Linehan DC. Immunologic strategies in pancreatic cancer: making cold tumors hot. J Clin Oncol 2022; 40: 2789-2805.

[16] Li YX, Zhu XX, Wu X, Li JH, Ni XH, Li SJ, Zhao W and Yin XY. ACLP promotes activation of cancer-associated fibroblasts and tumor metastasis via ACLP-PPARγ-ACLP feedback loop in pancreatic cancer. Cancer Lett 2022; 544: 215802.

[17] Sha D, Jin Z, Budczies J, Kluck K, Stenzinger A and Sinicrope FA. Tumor mutational burden as a predictive biomarker in solid tumors. Cancer Discov 2020; 10: 1808-1825.
[18] Samstein RM, Lee CH, Shoushtari AN, Hellmann MD, Shen R, Janjigian YY, Barron DA, Zehir A, Jordan EJ, Omuro A, Kaley TJ, Kendall SM, Motzer RJ, Hakimi AA, Voss MH, Russo P, Rosenberg J, Iyer G, Bochner BH, Bajorin DF, Al-Ahmadie HA, Chaft JE, Rudin CM, Riely GJ, Baxi S, Ho AL, Wong RJ, Pfister DG, Wolchok JD, Barker CA, Gutin PH, Brennan CW, Tabar V, Mellinghoff IK, DeAngelis LM, Ariyan CE, Lee N, Tap WD, Gounder MM, D'Angelo SP, Saltz L, Stadler ZK, Scher HI, Baselga J, Razavi P, Klebanoff CA, Yaeger R, Segal NH, Ku GY, DeMatteo RP, Ladanyi M, Rizvi NA, Berger MF, Riaz N, Solit DB, Chan TA and Morris LGT. Tumor mutational load predicts survival after immunotherapy across multiple cancer types. Nat Genet 2019; 51: 202-206.
[19] Goodman AM, Kato S, Bazhenova L, Patel SP, Frampton GM, Miller V, Stephens PJ, Daniels GA and Kurzrock R. Tumor mutational burden as an independent predictor of response to immunotherapy in diverse cancers. Mol Cancer Ther 2017; 16: 2598-2608.
[20] Lankadasari MB, Mukhopadhyay P, Mohammed S and Harikumar KB. TAMing pancreatic cancer: combat with a double edged sword. Mol Cancer 2019; 18: 48.
[21] Thakur A, Banerjee R, Thakur S, Kumar G and Thakur SS. Role of macrophage polarization in cancer progression and their association with COVID-19 severity. Cancer Insight 2023; 2: 68-79.
[22] Lin A, Qi C, Wei T, Li M, Cheng Q, Liu Z, Luo P and Zhang J. CAMOIP: a web server for comprehensive analysis on multi-omics of immunotherapy in pan-cancer. Brief Bioinform 2022; 23: bbac129.
[23] Ru B, Wong CN, Tong Y, Zhong JY, Zhong SSW, Wu WC, Chu KC, Wong CY, Lau CY, Chen I, Chan NW and Zhang J. TISIDB: an integrated repository portal for tumor-immune system interactions. Bioinformatics 2019; 35: 4200-4202.
[24] Park SJ, Yoon BH, Kim SK and Kim SY. GENT2: an updated gene expression database for normal and tumor tissues. BMC Med Genomics 2019; 12 Suppl 5: 101.
[25] Li T, Fan J, Wang B, Traugh N, Chen Q, Liu JS, Li B and Liu XS. TIMER: a web server for comprehensive analysis of tumor-infiltrating immune cells. Cancer Res 2017; 77: e108-e110.
[26] Li B, Severson E, Pignon JC, Zhao H, Li T, Novak J, Jiang P, Shen H, Aster JC, Rodig S, Signoretti S, Liu JS and Liu XS. Comprehensive analyses of tumor immunity: implications for cancer immunotherapy. Genome Biol 2016; 17: 174.
[27] Tang Z, Li C, Kang B, Gao G, Li C and Zhang Z. GEPIA: a web server for cancer and normal gene expression profiling and interactive analyses. Nucleic Acids Res 2017; 45: W98-W102.
[28] Hanzelmann S, Castelo R and Guinney J. GSVA: gene set variation analysis for microarray and RNA-seq data. BMC Bioinformatics 2013; 14: 7.
[29] Meng Q, Liang C, Hua J, Zhang B, Liu J, Zhang Y, Wei M, Yu X, Xu J and Shi S. A miR-146a-5p/TRAF6/NF-kB p65 axis regulates pancreatic cancer chemoresistance: functional validation and clinical significance. Theranostics 2020; 10: 3967-3979.
[30] Liu M, Zhang Y, Yang J, Cui X, Zhou Z, Zhan H, Ding K, Tian X, Yang Z, Fung KA, Edil BH, Postier RG, Bronze MS, Fernandez-Zapico ME, Stemmler MP, Brabletz T, Li YP, Houchen CW and Li M. ZIP4 Increases expression of transcription factor ZEB1 to promote integrin alpha3beta1 signaling and inhibit expression of the gemcitabine transporter ENT1 in pancreatic cancer cells. Gastroenterology 2020; 158: 679-692, e671.
[31] Yao Y, Liu C, Wang B, Guan X, Fang L, Zhan F, Sun H, Li H, Lou C, Yan F, Lu X, Cui L, Liao Y, Han S, Yao Y and Zhang Y. HOXB9 blocks cell cycle progression to inhibit pancreatic cancer cell proliferation through the DNMT1/RBL2/c-Myc axis. Cancer Lett 2022; 533: 215595.
[32] Peng J, Sun BF, Chen CY, Zhou JY, Chen YS, Chen H, Liu L, Huang D, Jiang J, Cui GS, Yang Y, Wang W, Guo D, Dai M, Guo J, Zhang T, Liao Q, Liu Y, Zhao YL, Han DL, Zhao Y, Yang YG and Wu W. Single-cell RNA-seq highlights intra-tumoral heterogeneity and malignant progression in pancreatic ductal adenocarcinoma. Cell Res 2019; 29: 725-738.
[33] Galon J and Bruni D. Approaches to treat immune hot, altered and cold tumours with combination immunotherapies. Nat Rev Drug Discov 2019; 18: 197-218.
[34] Li TJ, Jin KZ, Li H, Ye LY, Li PC, Jiang B, Lin X, Liao ZY, Zhang HR, Shi SM, Lin MX, Fei QL, Xiao ZW, Xu HX, Liu L, Yu XJ and Wu WD. SIGLEC15 amplifies immunosuppressive properties of tumor-associated macrophages in pancreatic cancer. Cancer Lett 2022; 530: 142-155.
[35] Balachandran VP, Luksza M, Zhao JN, Makarov V, Moral JA, Remark R, Herbst B, Askan G, Bhanot U, Senbabaoglu Y, Wells DK, Cary CIO, Grbovic-Huezo O, Attiyeh M, Medina B, Zhang J, Loo J, Saglimbeni J, Abu-Akeel M, Zappasodi R, Riaz N, Smoragiewicz M, Kelley ZL, Basturk O; Australian Pancreatic Cancer Genome Initiative; Garvan Institute of Medical Research; Prince of Wales Hospital; Royal North Shore Hospital; University of Glasgow; St Vincent's Hospital; QIMR Berghofer Medical Research

Institute; University of Melbourne, Centre for Cancer Research; University of Queensland, Institute for Molecular Bioscience; Bankstown Hospital; Liverpool Hospital; Royal Prince Alfred Hospital, Chris O'Brien Lifehouse; Westmead Hospital; Fremantle Hospital; St John of God Healthcare; Royal Adelaide Hospital; Flinders Medical Centre; Envoi Pathology; Princess Alexandria Hospital; Austin Hospital; Johns Hopkins Medical Institutes; ARC-Net Centre for Applied Research on Cancer, Gonen M, Levine AJ, Allen PJ, Fearon DT, Merad M, Gnjatic S, Iacobuzio-Donahue CA, Wolchok JD, DeMatteo RP, Chan TA, Greenbaum BD, Merghoub T and Leach SD. Identification of unique neoantigen qualities in long-term survivors of pancreatic cancer. Nature 2017; 551: 512-516.

[36] Uyttenhove C, Pilotte L, Theate I, Stroobant V, Colau D, Parmentier N, Boon T and Van den Eynde BJ. Evidence for a tumoral immune resistance mechanism based on tryptophan degradation by indoleamine 2,3-dioxygenase. Nat Med 2003; 9: 1269-1274.

[37] Bayne LJ, Beatty GL, Jhala N, Clark CE, Rhim AD, Stanger BZ and Vonderheide RH. Tumor-derived granulocyte-macrophage colony-stimulating factor regulates myeloid inflammation and T cell immunity in pancreatic cancer. Cancer Cell 2012; 21: 822-835.

[38] Coelho MA, de Carne Trecesson S, Rana S, Zecchin D, Moore C, Molina-Arcas M, East P, Spencer-Dene B, Nye E, Barnouin K, Snijders AP, Lai WS, Blackshear PJ and Downward J. Oncogenic RAS signaling promotes tumor immunoresistance by stabilizing PD-L1 mRNA. Immunity 2017; 47: 1083-1099, e1086.

[39] Yamamoto K, Venida A, Yano J, Biancur DE, Kakiuchi M, Gupta S, Sohn ASW, Mukhopadhyay S, Lin EY, Parker SJ, Banh RS, Paulo JA, Wen KW, Debnath J, Kim GE, Mancias JD, Fearon DT, Perera RM and Kimmelman AC. Autophagy promotes immune evasion of pancreatic cancer by degrading MHC-I. Nature 2020; 581: 100-105.

[40] McCracken MN, Cha AC and Weissman IL. Molecular pathways: activating T cells after cancer cell phagocytosis from blockade of CD47 "Don't Eat Me" signals. Clin Cancer Res 2015; 21: 3597-3601.

[41] Kadomoto S, Izumi K and Mizokami A. The CCL20-CCR6 axis in cancer progression. Int J Mol Sci 2020; 21: 5186.

[42] van der Woude LL, Gorris MAJ, Halilovic A, Figdor CG and de Vries IJM. Migrating into the tumor: a roadmap for T cells. Trends Cancer 2017; 3: 797-808.

[43] Nolz JC. Molecular mechanisms of CD8(+) T cell trafficking and localization. Cell Mol Life Sci 2015; 72: 2461-2473.

[44] Chen K, Wang Y, Hou Y, Wang Q, Long D, Liu X, Tian X and Yang Y. Single cell RNA-seq reveals the CCL5/SDC1 receptor-ligand interaction between T cells and tumor cells in pancreatic cancer. Cancer Lett 2022; 545: 215834.

[45] Peran I, Dakshanamurthy S, McCoy MD, Mavropoulos A, Allo B, Sebastian A, Hum NR, Sprague SC, Martin KA, Pishvaian MJ, Vietsch EE, Wellstein A, Atkins MB, Weiner LM, Quong AA, Loots GG, Yoo SS, Assefnia S and Byers SW. Cadherin 11 promotes immunosuppression and extracellular matrix deposition to support growth of pancreatic tumors and resistance to gemcitabine in mice. Gastroenterology 2021; 160: 1359-1372, e1313.

[46] Garcia Garcia CJ, Huang Y, Fuentes NR, Turner MC, Monberg ME, Lin D, Nguyen ND, Fujimoto TN, Zhao J, Lee JJ, Bernard V, Yu M, Delahoussaye AM, Jimenez Sacarello I, Caggiano EG, Phan JL, Deorukhkar A, Molkentine JM, Saur D, Maitra A and Taniguchi CM. Stromal HIF2 regulates immune suppression in the pancreatic cancer microenvironment. Gastroenterology 2022; 162: 2018-2031.

Table S1. The number of tumor and normal samples from TCGA and GTEx database

Types	TCGA-Tumor	TCGA-Normal	GTEx-Type	GTEx-Normal	Total-Tumor	Total-Normal
ACC	77	0	Adrenal Gland	128	77	128
BLCA	404	19	Bladder	9	404	28
BRCA	1085	112	Breast	179	1085	291
CESC	306	3	Cervix Uteri	10	306	13
CHOL	36	9	NA	NA	36	9
COAD	275	41	Colon	308	275	349
DLBC	47	0	Blood	337	47	337
ESCA	182	13	Esophagus	273	182	286
GBM	163	0	Brain	207	163	207
HNSC	519	44	NA	NA	519	44
KICH	66	25	Kidney	28	66	53
KIRC	523	72	Kidney	28	523	100
KIRP	286	32	Kidney	28	286	60
LAML	173	0	Bone Marrow	70	173	70
LGG	518	0	Brain	207	518	207
LIHC	369	50	Liver	110	369	160
LUAD	483	59	Lung	288	483	347
LUSC	486	50	Lung	288	486	338
MESO	87	0	NA	NA	87	0
OV	426	0	Ovary	88	426	88
PAAD	179	4	Pancreas	167	179	171
PCPG	182	3	NA	NA	182	3
PRAD	492	52	Prostate	100	492	152
READ	92	10	Colon	308	92	318
SARC	262	2	NA	NA	262	264
SKCM	461	1	Skin	557	461	558
STAD	408	36	Stomach	175	408	211
TGCT	137	0	Testis	165	137	165
THCA	512	59	Thyroid	278	512	337
THYM	118	2	Blood	337	118	339
UCEC	174	13	Uterus	78	174	91
UCS	57	0	Uterus	78	57	78
UVM	79	0	NA	NA	79	0

Table S2. Sequences of the oligonucleotides for shRNA, and real-time PCR (5'-3')

Quantitative PCR	
GAPDH(F)	GGAGCGAGATCCCTCCAAAAT
GAPDH(R)	GGCTGTTGTCATACTTCTCATGG
PCDH1(F)	ACGCCACTCGGGTAGTGTA
PCDH1(R)	TCACGGTCGATGGAGGTCTC
CCL5(F)	CCAGCAGTCGTCTTTGTCAC
CCL5(R)	CTCTGGGTTGGCACACACTT
CCR5(F)	TTCTGGGCTCCCTACAACATT
CCR5(R)	TTGGTCCAACCTGTTAGAGCTA
Construction of shRNA vector	
PCDH1-SH1	GCTGAGCTGATCTACAGCATT
PCDH1-SH2	GGGAGTGATGGAGCAGGTTTA
PCDH1-SH3	GCTCTAATGCTGAGCTGGTTT
PCDH1-SHNC	CCTAAGGTTAAGTCGCCCTCG

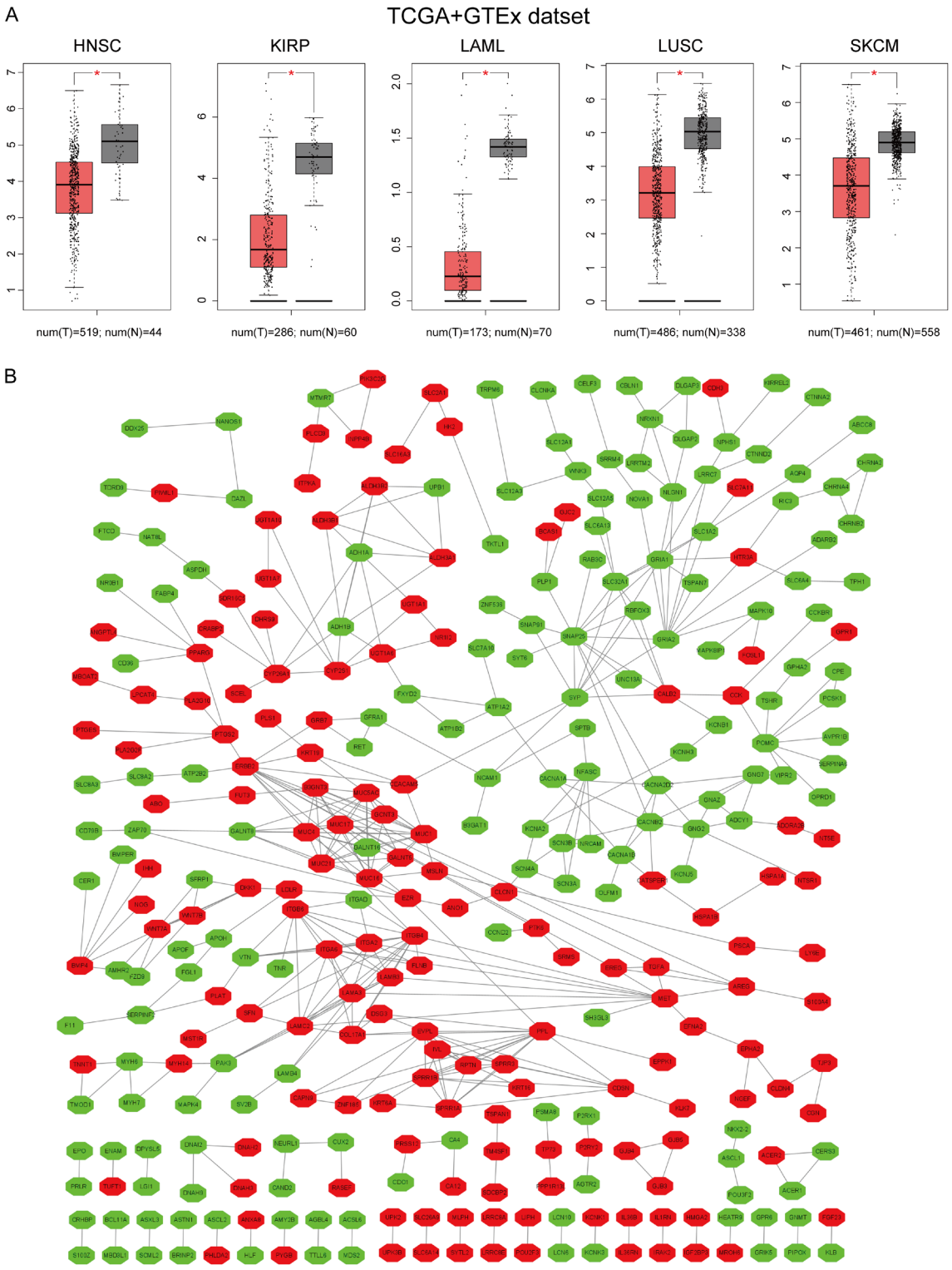

Figure S1. A: PCDH1 expression across various cancer types. B: PPI analysis of differentially expressed genes in high and low expression group of PCDH1 (The red squares are up-regulated genes in the PCDH1 high expression group, and the green squares are down-regulated genes in the PCDH1 high expression group).

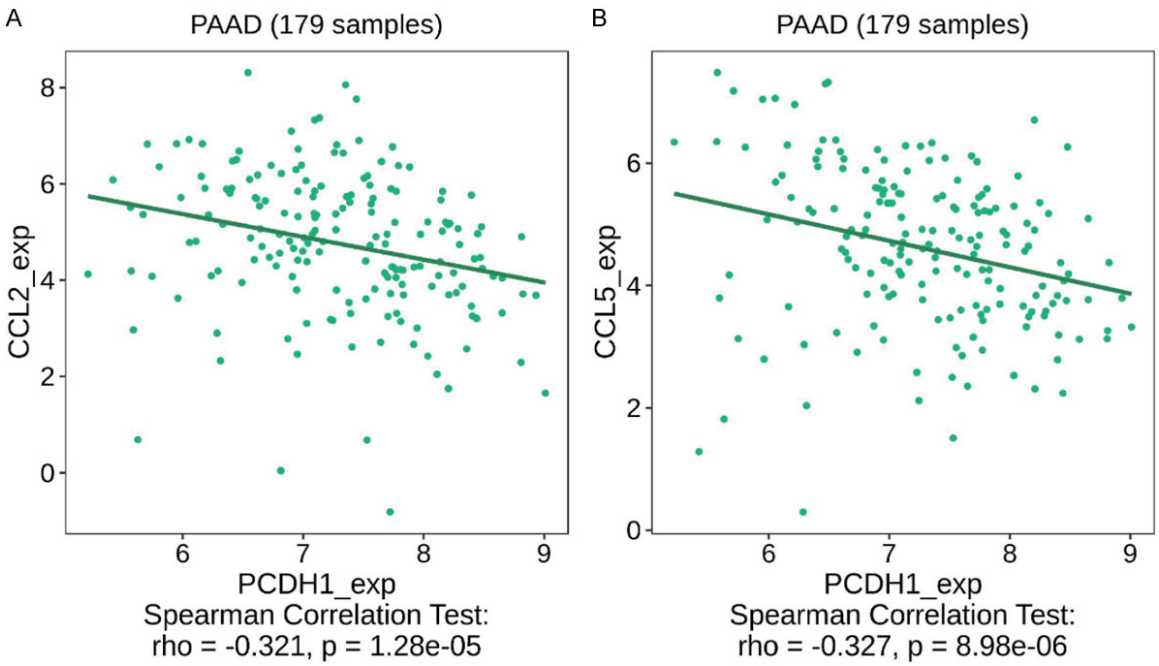

Figure S2. A: In TCGA-PAAD, the PCDH1 expression was negatively correlated with the CCL2 expression (R=-0.321; *P*=1.28e-05). B: In TCGA-PAAD, the PCDH1 expression was negatively correlated with the CCL5 expression (R=-0.327; *P*=8.98e-06).